

Breaking up the Proton: An Affair with Dark Forces

Graham D. Kribs,^{1,*} David McKeen,^{2,†} and Nirmal Raj^{2,‡}

¹*Institute for Fundamental Science and Department of Physics, University of Oregon, Eugene, OR 97403, USA*

²*TRIUMF, 4004 Wesbrook Mall, Vancouver, BC V6T 2A3, Canada*

(Dated: January 26, 2022)

Deep inelastic scattering of e^\pm off protons is sensitive to contributions from “dark photon” exchange. Using HERA data fit to HERA’s parton distribution functions, we obtain the model-independent bound $\epsilon \lesssim 0.02$ on the kinetic mixing between hypercharge and the dark photon for dark photon masses $\lesssim 10$ GeV. This slightly improves on the bound obtained from electroweak precision observables. For higher masses the limit weakens monotonically; $\epsilon \lesssim 1$ for a dark photon mass of 5 TeV. Utilizing PDF sum rules, we demonstrate that the effects of the dark photon cannot be (trivially) absorbed into re-fit PDFs, and in fact lead to non-DGLAP (Bjorken x_B -independent) scaling violations that could provide a smoking gun in data. The proposed $e^\pm p$ collider operating at $\sqrt{s} = 1.3$ TeV, LHeC, is anticipated to accumulate 10^3 times the luminosity of HERA, providing substantial improvements in probing the effects of a dark photon: sensitivity to ϵ well below that probed by electroweak precision data is possible throughout virtually the entire dark photon mass range, as well as being able to probe to much higher dark photon masses, up to 100 TeV.

Introduction.

Are there new gauge interactions in Nature? A new, massive abelian vector boson (“dark photon”) can, at the renormalizable level, mix kinetically with the Standard Model hypercharge boson [1]:

$$\mathcal{L} \supset \frac{\epsilon}{2 \cos \theta_W} F'_{\mu\nu} B^{\mu\nu} . \quad (1)$$

Kinetic mixing with the hypercharge gauge boson becomes, after electroweak symmetry breaking, mixing of the dark photon with the neutral weak boson of the Standard Model (SM). We denote the unmixed dark photon by A'_μ and the unmixed neutral weak boson by \bar{Z} . Diagonalizing the Lagrangian kinetic terms and gauge boson mass matrix results in three physical vectors that couple to SM fermions: the massless photon γ , and the mass eigenstates Z and A_D .

Numerous searches for the dark photon have been undertaken by directly producing it, in which case the signature depends on its decay mode. In the minimal setup where the only relevant couplings come from Eq. (1), the dark photon decays back into charged standard model states, e.g. lepton pairs, offering striking signatures. However, the coupling in Eq. (1) may serve as our portal to a hidden sector that contains the particle species of the enigmatic dark matter [2, 3], and in this case the dark photon might decay invisibly or in a more complicated way depending on the structure of the hidden sector. It is therefore desirable to have “decay-agnostic” bounds that are independent of the details of a hidden sector.

In this study, we investigate one such decay-agnostic process: deep inelastic scattering (DIS) of e^\pm off protons. As seen in the Feynman diagram in Fig. 1, DIS in the

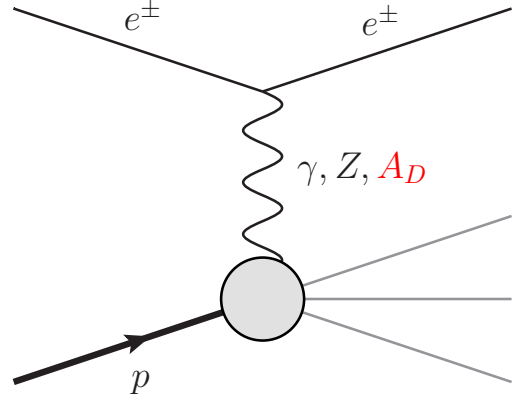


FIG. 1. Deep inelastic scattering of e^\pm on the proton, mediated by the Standard Model photon and Z boson, and a dark photon arising from kinetic mixing with an abelian hidden sector. Measurements of this process at HERA and LHeC probe the mixing parameter and dark photon mass without relying on any assumptions about the production and decay properties of A_D .

presence of kinetic mixing is mediated by the photon, the Z , and the dark photon A_D . A_D exchange leads to distinct non-DGLAP scaling violations that may be constrained by existing data and may also be the smoking gun of a dark photon in future experiments.

Dark photon decay-agnostic limits on kinetic mixing were obtained in Refs. [4, 5] from electroweak precision observables (EWPO), driven mainly by the 0.1% precision Z pole-mass measurements at LEP. The main effect is a shift of the Z mass relative to $m_W / \cos \theta_W$, and using a global fit to EWPO, a bound of $\epsilon \lesssim 0.03$ was obtained for $m_{A_D} \ll m_Z$. We show that DIS measurements at the $e^\pm p$ collider HERA can improve on this bound. With a net luminosity of 1 fb^{-1} , HERA achieved 1% (systematics-limited) precision, however multiple measurements at

* kribs@uoregon.edu

† mckeen@triumf.ca

‡ nrj@triumf.ca

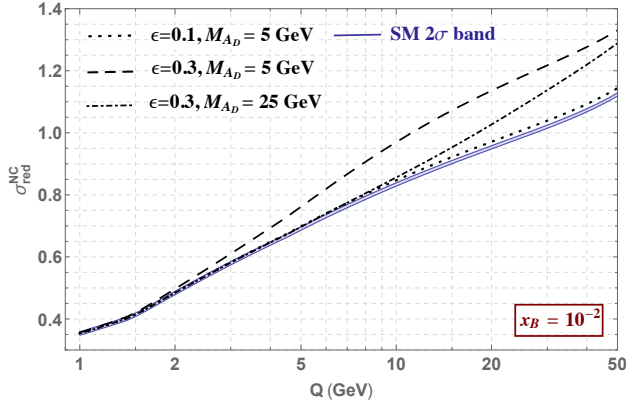


FIG. 2. DIS neutral-current reduced cross sections for a representative Bjorken variable $x_B = 10^{-2}$, as estimated in Eq. (4) using HERAPDF2.0 LO. The blue band covers 2σ uncertainties in the SM cross section, obtained by using PDF uncertainties and summing in quadrature the terms in Eq. (4). In this regime where $Q \ll m_Z$, the effects of Z are negligible and A_D behaves like a massive photon constructively interfering with the SM photon, leading to cross sections scaled by a factor of $1 + 2\epsilon^2 Q^2 / (Q^2 + m_{A_D}^2)$ relative to the SM. Importantly, the cross sections at all Bjorken x_B values experience a shift *at the same* $|Q| \sim m_{A_D}$ that is a non-DGLAP scaling violation of the cross sections, providing a prominent feature of the contribution from a dark photon. Already the $\epsilon = 0.1$ curve can be visually distinguished from the SM, and when combined with the plethora of measurements at other x_B values, it is clear that DIS at HERA can probe the considerably smaller values of $\epsilon \simeq 0.02$ as we show in Fig. 3.

this precision give additional statistical power. Decay-agnostic constraints also arise from measurements of the muon’s anomalous magnetic moment, which receives contributions from A_D -mediated loop amplitudes [6]; these limits however weaken considerably for A_D masses above the muon mass, becoming negligible above 10 GeV. On the other hand, we show that DIS can probe dark photon masses of 10^4 GeV and beyond.

As discussed above, if assumptions are made about the decay modes of the dark photon, additional constraints apply that may be considerably stronger in the region $m_{A_D} < 10$ GeV. See Refs. [3, 7, 8] for a review of these constraints arising from colliders, beam dump experiments, and other probes.

Signals of kinetic mixing in deep inelastic scattering.

In this section we review the basics of deep inelastic scattering, incorporating dark photon exchange (for reviews, see e.g. [9–11]). DIS is described by the Lorentz-invariant kinematic variables

$$Q^2 = -q^2, \quad x_B = \frac{Q^2}{2q \cdot p}, \quad y = \frac{q \cdot p}{k \cdot p}, \quad (2)$$

where q is the momentum transfer and p (k) is the incoming proton’s (electron’s) momentum. Using these kinematic

variables, the unpolarized neutral-current differential cross section rescaled as a (dimensionless) “reduced cross section” $\sigma_{\text{red}}^{\text{NC}}$ is:

$$\sigma_{\text{red}}^{\text{NC}} = \frac{Q^4 x_B}{2\pi\alpha^2 [1 + (1 - y)^2]} \frac{d^2\sigma}{dx_B dQ^2}. \quad (3)$$

The cross section can be expressed in terms of the parton distribution functions (PDFs) as per the QCD factorization theorem. In the Quark Parton Model (QPM), DIS proceeds via elastic scattering on point-like quarks and anti-quarks, hence their PDFs f_q alone contribute and the variable x_B becomes the momentum fraction of the proton carried by the parton in the infinite momentum frame; moreover longitudinal effects are negligible. Neglecting parity-violating effects, $\sigma_{\text{red}}^{\text{NC}}$ is equal to the structure function:

$$\tilde{F}_2 = \sum_{i,j=\gamma,Z,A_D} \kappa_i \kappa_j F_2^{ij}, \quad (4)$$

where $\kappa_i = Q^2 / (Q^2 + M_{V_i}^2)$ accounts for the propagators of vector bosons of mass M_{V_i} . At leading order¹ in α_s ,

$$F_2^{ij} = \sum_q x_B f_q (C_{i,e}^v C_{j,e}^v + C_{i,e}^a C_{j,e}^a) (C_{i,q}^v C_{j,q}^v + C_{i,q}^a C_{j,q}^a),$$

where the summation runs over $q = u, \bar{u}, d, \bar{d}, c, \bar{c}, s, \bar{s}, b, \bar{b}$, and the vector and axial couplings to fermions (in units of $e = \sqrt{4\pi\alpha}$) are given as follows: For the SM photon,

$$\{C_{\gamma,e}^v, C_{\gamma,u}^v, C_{\gamma,d}^v\} = \left\{-1, \frac{2}{3}, -\frac{1}{3}\right\}, \quad C_{\gamma}^a = 0. \quad (5)$$

For the unmixed \bar{Z} boson,

$$\bar{C}_Z^v \sin 2\theta_W = T_3^f - 2q_f \sin^2 \theta_W, \quad \bar{C}_Z^a \sin 2\theta_W = T_3^f, \quad (6)$$

where $\{T_3^e, T_3^u, T_3^d\} = \{-1/2, 1/2, -1/2\}$ is the weak isospin, $\{q_e, q_u, q_d\} = \{-1, 2/3, -1/3\}$ is the electric charge, and the usual Weinberg angle $\sin^2 \theta_W \simeq 0.23127$ [13].

We can now add the effects of dark photon exchange. First we diagonalize the A' mixing with hypercharge shown in Eq. (1) through the field redefinition:

$$B_\mu \rightarrow B_\mu + \frac{\epsilon}{\cos \theta_W} A'_\mu, \quad (7)$$

and canonically normalize the resulting dark photon kinetic term through the field rescaling:

$$A'_\mu \rightarrow \frac{A'_\mu}{\sqrt{1 - \epsilon^2 / \cos^2 \theta_W}}. \quad (8)$$

¹ By using the QCD factorization theorem at next-to-leading order (NLO) and by using NLO PDFs derived by HERA, we have checked that treating the problem at NLO gives quite similar results. As discussed in Ref. [12], while fitting PDFs their uncertainties remain roughly the same as one goes to higher orders in α_s .

In the $\epsilon \rightarrow \cos \theta_W$ limit the rescaling of A'_μ results in the enhancement of the dark gauge coupling, simultaneously enhancing couplings to SM fermion currents. This in turn increases our sensitivity to large m_{A_D} .

The dark photon and \bar{Z} squared mass matrix becomes

$$M^2 = \bar{m}_Z^2 \begin{bmatrix} 1 & -\epsilon_W \\ -\epsilon_W & \epsilon_W^2 + \rho^2 \end{bmatrix}, \quad (9)$$

where

$$\begin{aligned} \epsilon_W &= \frac{\epsilon \tan \theta_W}{\sqrt{1 - \epsilon^2 / \cos^2 \theta_W}}, \\ \rho &= \frac{\bar{m}_{A'} / \bar{m}_Z}{\sqrt{1 - \epsilon^2 / \cos^2 \theta_W}}, \end{aligned} \quad (10)$$

and the \bar{Z} - A' mixing angle is given by

$$\begin{aligned} \tan \alpha &= \frac{1}{2\epsilon_W} \left[1 - \epsilon_W^2 - \rho^2 \right. \\ &\quad \left. - \text{sign}(1 - \rho^2) \sqrt{4\epsilon_W^2 + (1 - \epsilon_W^2 - \rho^2)^2} \right]. \end{aligned} \quad (11)$$

The physical Z couplings are

$$\begin{aligned} C_Z^v &= (\cos \alpha - \epsilon_W \sin \alpha) \bar{C}_Z^v + \epsilon_W \sin \alpha \cot \theta_W C_\gamma^v, \\ C_Z^a &= (\cos \alpha - \epsilon_W \sin \alpha) \bar{C}_Z^a, \end{aligned} \quad (12)$$

while those of the physical A_D are

$$\begin{aligned} C_{A_D}^v &= -(\sin \alpha + \epsilon_W \cos \alpha) \bar{C}_Z^v + \epsilon_W \cos \alpha \cot \theta_W C_\gamma^v, \\ C_{A_D}^a &= -(\sin \alpha + \epsilon_W \cos \alpha) \bar{C}_Z^a. \end{aligned} \quad (13)$$

The masses of the physical states are

$$\begin{aligned} m_{Z, A_D}^2 &= \frac{m_Z^2}{2} \left[1 + \epsilon_W^2 + \rho^2 \right. \\ &\quad \left. \pm \text{sign}(1 - \rho^2) \sqrt{(1 + \epsilon_W^2 + \rho^2)^2 - 4\rho^2} \right]. \end{aligned} \quad (14)$$

Note that for fixed ϵ and any value of $\bar{m}_{A'} / \bar{m}_Z$ the difference between the Z and A_D masses is always finite, $|m_Z^2 - m_{A_D}^2| \geq 2|\epsilon_W| m_Z^2$. This ‘‘eigenmass repulsion’’, a well-known property of real symmetric matrices (including M^2) that implies that there are regions of the ϵ - m_{A_D} plane that cannot be realized.

Note that the cross section in Eq. (4) is invariant under $\epsilon \rightarrow -\epsilon$. This arises from requiring A' to couple to both quark and lepton currents to be observable at DIS, so that deviations from the SM cross section arise first at $\mathcal{O}(\epsilon^2)$.

For $Q^2 \ll m_Z^2$, the short-distance Z -exchange is negligible, and A_D modifies the DIS cross section mainly through its constructive interference with the SM photon. Thus it effectively rescales the cross section by a factor of $[1 + \epsilon^2 Q^2 / (Q^2 + m_{A_D}^2)]^2$ in this regime. We illustrate this in Fig. 2 where we plot, for a representative $x_B = 10^{-2}$, $\sigma_{\text{red}}^{\text{NC}}$ versus Q for $\epsilon = 0$ as a band covering 2σ uncertainties, and for $(\epsilon, m_{A_D}/\text{GeV}) = (0.1, 5)$, $(0.3, 5)$, and $(0.3,$

25). Clearly larger ϵ values produce larger effects; more subtly, m_{A_D} sets the scale in Q above which the effects of A_D become significant. Note that the $\epsilon = 0.1$ curve lies well outside the SM band, indicating that HERA can probe $\epsilon \ll 0.1$ with a dataset spanning multiple x_B .

For $Q \gg m_Z$ DIS probes the regime of unbroken electroweak symmetry, where the SM process transpires effectively via massless B exchange. As we will see in the next section, here too the effect of kinetic mixing is to rescale the cross section by $[1 + \epsilon^2 Q^2 / (Q^2 + m_{A_D}^2)]^2$.

HERA constraints and LHeC sensitivities.

To constrain kinetic mixing with DIS, we use the combined datasets of Runs I and II at HERA [12] over the ranges

$$0.15 \leq Q^2/\text{GeV}^2 \leq 3 \times 10^4, \quad 5 \times 10^{-6} \leq x_B \leq 0.65.$$

In principle, our constraints must be obtained fitting the HERA data simultaneously to both the dark photon parameters (ϵ, m_{A_D}) and the PDFs f_q . In practice, however, we only fit to the dark photon parameters,² and use the HERAPDF2.0 LO PDF set derived in Ref. [12] (importing it into Mathematica via ManeParse2.0 [14]).

We believe the bounds we obtain from this simplified approach are, in fact, robust against performing a simultaneous fit. Let us justify this. First consider the region $m_{A_D} \ll Q_{\text{min}}$, where Q_{min} is the smallest Q probed at HERA. The cross sections in Eq. (4) are rescaled by $(1 + \epsilon^2)^2$ with respect to the SM, as discussed in the previous section. This implies that the PDFs could absorb this rescaling of the cross section by a simultaneous rescaling of all quark flavors, c.f. Eq. (4). However the normalization of f_q is constrained by PDF sum rules. The quark-number sum rules

$$\int dx_B [f_q(x_B) - f_{\bar{q}}(x_B)] = \begin{cases} 2, & q = u, \\ 1, & q = d, \\ 0, & q = s, c, b, \end{cases}$$

and the momentum sum rule

$$\int dx_B x_B \left[\sum_q f_q(x_B) + f_g(x_B) \right] = 1, \quad (15)$$

applied over the HERA Q range are satisfied to $\mathcal{O}(10^{-4})$ precision. Using additional data in ranges of Q^2 outside HERA’s, such as from beam dumps and hadron colliders, the sum rules can be further constrained once DGLAP evolution is accounted for.

² Our procedure can be viewed as estimating the expected sensitivities on our model using a second dataset with the same (Q^2, x_B) grid as HERA, with PDFs fitted under the Standard Model null hypothesis. This is precisely what we do when we estimate the sensitivity of LHeC below.

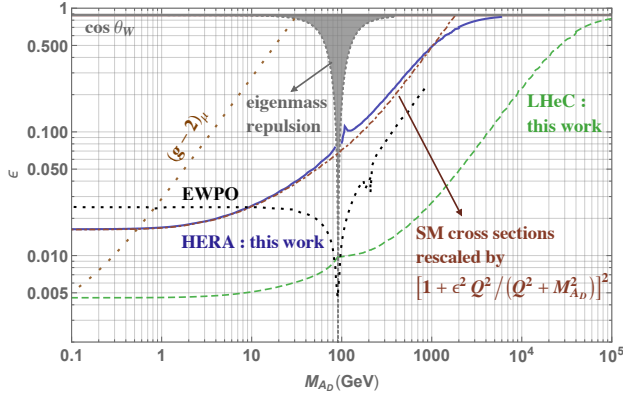


FIG. 3. 95% C.L. limits on the kinetic mixing parameter vs dark photon mass from deep inelastic scattering (DIS) measurements. Shown are limits from HERA derived using HERAPDF2.0 LO sets, and future sensitivities at LHeC, using PDF4LHC15_NNLO_LHEC PDFs. For comparison are shown other decay-agnostic limits from measurements of electroweak precision observables (EWPO) and the muon $g-2$. Also shown are hypothetical limits obtained by rescaling SM DIS cross sections by a factor of $[1 + \epsilon^2 Q^2 / (Q^2 + m_{A_D}^2)]^2$, amounting to accounting only for interference between A_D and B boson exchange. In the gray-shaded region there is no physical value of m_{A_D} in the neighborhood of $m_Z = 91.1876$ GeV due to repulsion of eigenmasses. The change in slope shift of the HERA and LHeC sensitivity curves at large $\epsilon \gtrsim 0.7$ and $m_{A_D} \gtrsim 1$ TeV occurs due to a factor of $1/\sqrt{1 - \epsilon^2/\cos^2\theta_W}$ enhancement in the dark photon-fermion coupling. See text for further details.

Next, consider the parameter region where m_{A_D} is large compared with the momentum exchange for DIS. In this regime, the dark photon can be integrated out, resulting in a rescaled cross section $[1 + \epsilon^2 Q^2 / (Q^2 + m_{A_D}^2)]^2 \simeq 1 + 2\epsilon^2 Q^2 / m_{A_D}^2$. The Q^2 polynomial growth in the rescaled cross section leads to the largest corrections near $Q^2 \sim m_{A_D}^2$, i.e. near the edge of validity of the effective field theory. Reference [15] showed that integrating out new particles at 250 GeV that led to modified quark-lepton interactions could be mostly disentangled from the logarithmic scaling of DGLAP evolution. That is, the new physics effects could not be easily “fitted away” into the PDFs.

Finally, for $Q_{\min} < m_{A_D} < Q_{\max}$, there is a (smoothed out) step in the rescaled cross section at $Q \simeq m_{A_D}$ which comes from the factor of $[1 + \epsilon^2 Q^2 / (Q^2 + m_{A_D}^2)]^2$, illustrated in Fig. 2. Since this step occurs at the same Q^2 for all x_B values, it also does not behave like DGLAP evolution.

In order to obtain the net uncertainty in $\sigma_{\text{red}}^{\text{NC}}$, we use the HERAPDF uncertainties to sum in quadrature the uncertainties of the terms in Eq. (4). It is these uncertainties that we will use to estimate our limits, as opposed to the errors in the “raw” measurements of the cross sections, since (a) the covariance matrix describing correlations among the errors is not given, and (b) the PDF fitting procedure accounts for these correlations.

In deriving our bounds, we use the (Q^2, x_B) grid used for the HERA run involving e^+ scattering with $\sqrt{s} = 318$ GeV and 0.5 fb^{-1} luminosity, as given in Table 10 of Ref. [12]. This grid, containing 485 points, covers most of the (Q^2, x_B) used in the other runs involving e^\pm scattering at smaller \sqrt{s} and luminosity; although data from all these runs were used for fitting PDFs, we do not use these other grids to avoid oversampling. We derive the 95% C.L. limit by locating values of (ϵ, m_{A_D}) for which

$$\chi^2 = \sum_{\text{grid}} \frac{(\sigma_{\text{red}}^{\text{NC}} - \sigma_{\text{red}}^{\text{NC}}|_{\epsilon \rightarrow 0})^2}{(\delta\sigma_{\text{red}}^{\text{NC}})^2} = 5.99, \quad (16)$$

where the summation is over the (Q^2, x_B) grid mentioned above. The resulting limits are displayed in Fig. 3. We also show the decay-agnostic limits from the $(g-2)_\mu$ measurement at the E821 experiment, requiring 5σ deviation from the central value using the calculations in Ref. [6], as well as the limits from EWPO derived in Ref. [4]. Our bounds are driven largely by about 25 data points in the (Q^2, x_B) grid where the cross section is obtained with a maximum precision of 0.3%-0.4%. This is the origin of why our limits are (slightly) stronger than EWPO for $m_{A_D} \lesssim 10 \text{ GeV} \ll m_Z$. In this regime the observable correction at both LEP Z pole measurements and DIS scales as ϵ^2 , and while LEP operated at a precision of 0.1%, which appears better than our precision, our bound actually benefits from 25 independent measurements, effectively diminishing our uncertainty by a statistical factor of $\sqrt{25}$. We also display a hypothetical bound obtained by simply rescaling the SM cross sections by $1 + 2\epsilon^2 Q^2 / (Q^2 + m_{A_D}^2)$, seen to trail the actual bound with amusing proximity. As discussed earlier, such a rescaling amounts to accounting only for A_D interference with the B exchange amplitude: for $Q \ll m_Z$ this effectively rescales photon exchange, and for higher Q it rescales both photon and Z exchange.

In this figure we also show the 95% C.L. sensitivity of the future $e^\pm p$ collider LHeC [16] derived by using the (Q^2, x_B) grid for e^+ scattering over the range

$$5 \leq Q^2/\text{GeV}^2 \leq 10^6, \quad 5 \times 10^{-6} \leq x_B \leq 0.8.$$

The LHeC is anticipated to obtain 10^3 times the integrated luminosity of HERA, thus gaining in statistical precision by a factor of about 30. We are interested in characterizing the maximal sensitivity that LHeC could achieve with this increased precision. This is a different objective from obtaining the best-fit PDFs across all datasets. Therefore, to estimate LHeC sensitivity, we use PDF4LHC15_NNLO_LHEC PDFs fitted to pseudo-data Ref. [17], but then rescale the fractional uncertainties to match with $\sqrt{1/10^3}$ times the fractional uncertainties of HERAPDF2.0 LO, optimistically assuming that systematic errors can be kept below this level. We have checked that rescaling the Q^2 values of the HERA grid by a factor of $5/0.15 = 10^6/(3 \times 10^4)$, the envelopes of smallest uncertainties (as a function of Q^2) for either PDF set are well-aligned. We see from the figure that LHeC exceeds

HERA in the entire m_{A_D} range constrained by the latter, and indeed reaches m_{A_D} up to 100 TeV thanks to probing the proton at very high Q .

The HERAPDF2.0 LO PDF set is designed to fit solely the HERA DIS data. We used this set not because we believe this is the best description of the quark PDFs, but because this is the most accurate interpolated description of the HERA data. Since we are interested in the sensitivity of HERA alone to kinetic mixing, we believe this is the correct approach to obtain the most accurate estimate of the sensitivity. We point out, however, that a more wide-ranging description of PDFs require “global fits” to DIS at HERA combined with beam-dump and hadron collider experiment datasets that include complementary ranges of Q^2 and x_B . Such PDF determinations contain additional sources of uncertainty [11]: (1) a “tolerance” factor to rescale the goodness-of-fit so that tensions in fitting multiple datasets may be eased to within 1σ uncertainty, (2) parameterization uncertainties introduced by the need to use numerous parameters to fit numerous datasets. The combination of these effects significantly increases the PDF uncertainties. Indeed we find that, had we used the global PDF set CT18Z [18], our bounds on ϵ would be weakened by a factor of up to 3. We do not believe this is a fair characterization of HERA’s bounds on kinetic mixing.

Finally, we note that EWPO sensitivities on ϵ are expected to improve by $\mathcal{O}(1)$ factors (a factor of ~ 10) with increased sensitivities provided by future LHC (ILC in GigaZ mode) measurements [5].

DIS-cussion.

Deep inelastic scattering of e^\pm off protons is a sensitive, model-independent probe of kinetic mixing with a dark photon up to 100 TeV masses. No assumptions need to be made regarding the dark photon’s decay modes. We find HERA data is slightly more sensitive than EWPO for dark photon masses less than about 10 GeV. The LHeC could significantly improve the sensitivity of DIS to kinetic mixing, probing values of ϵ well below the sensitivity of EWPO data.

It is intriguing to consider the possibility of *discovering* a dark photon’s signature in DIS data. This seems quite unlikely with existing HERA data, since EWPO leads to a stronger constraint for most of the parameter space. The main constraint from EWPO arises due to a shift of m_Z

relative to $m_W/\cos\theta_W$. It is possible, though unlikely, that other physics in the dark sector could compensate for this apparent contribution to custodial violation and weaken the EWPO bounds. In addition, the parameter region $m_{A_D} \lesssim 10$ GeV where DIS is slightly more sensitive is strongly constrained by *model-dependent* searches, especially from B -factories. In particular, the BaBar collaboration has searched for dark photons produced via $e^+e^- \rightarrow \gamma A_D$ assuming that A_D decays visibly through its kinetic mixing [19] or invisibly into a dark sector [20]. In both cases limits on ϵ at the level of 10^{-3} are obtained. A similar search by LHCb in the $\mu^+\mu^-$ final state constrains dark photons to $\epsilon \lesssim \mathcal{O}(10^{-3})$ up to 70 GeV masses [21]. These limits can potentially be weakened if A_D couples to a dark sector with further structure, leading to more complicated final states as in, e.g., [22].

The LHeC’s sensitivity is significantly better than EWPO, and this provides the most exciting possibility to directly search for the non-DGLAP (Bjorken x_B -independent) scaling violation in the cross section illustrated in Fig. 2. Maximizing the sensitivity would be best optimized by simultaneously fitting the PDFs with dark photon exchange. Nevertheless, we have emphasized that PDF sum rules provide strong constraints on “fitting away” the effects of a dark photon on PDFs, and other studies [15] have also found that PDFs do not easily fit away the polynomial scaling exhibited by massive dark photons.

In this study we have focused on the effects of a dark photon on DIS, however this can also be extended to any new force between quarks and leptons, such as mediated by a gauged $U(1)_{B-L}$ vector boson, new scalars in the Higgs sector, or other exotic force carriers. We leave these investigations to future work.

Acknowledgments. We are grateful to Paddy Fox, David Morrissey, John Ng, Maxim Pospelov, Tim Tait, Yue Zhao, and especially Dave Soper for beneficial conversations. The work of G.D.K. is supported in part by the U.S. Department of Energy under Grant Number DE-SC0011640. The work of D.M. and N.R. is supported by the Natural Sciences and Engineering Research Council of Canada. TRIUMF receives federal funding via a contribution agreement with the National Research Council Canada. This work was performed in part at the Aspen Center for Physics, which is supported by National Science Foundation grant PHY-1607611.

[1] L. Okun, Sov. Phys. JETP **56**, 502 (1982); P. Galison and A. Manohar, Phys. Lett. B **136**, 279 (1984); B. Holdom, Phys. Lett. **166B**, 196 (1986).
[2] M. Pospelov, A. Ritz, and M. B. Voloshin, Phys. Lett. **B662**, 53 (2008), arXiv:0711.4866 [hep-ph].
[3] R. Essig *et al.*, “Dark sectors and new, light, weakly-coupled particles,” (2013), arXiv:1311.0029 [hep-ph].
[4] A. Hook, E. Izaguirre, and J. G. Wacker, Adv. High En-

ergy Phys. **2011**, 859762 (2011), arXiv:1006.0973 [hep-ph].
[5] D. Curtin, R. Essig, S. Gori, and J. Shelton, JHEP **02**, 157 (2015), arXiv:1412.0018 [hep-ph].
[6] M. Pospelov, Phys. Rev. **D80**, 095002 (2009), arXiv:0811.1030 [hep-ph].
[7] P. Ilten, Y. Soreq, M. Williams, and W. Xue, JHEP **06**, 004 (2018), arXiv:1801.04847 [hep-ph].

- [8] M. Fabbrichesi, E. Gabrielli, and G. Lanfranchi, “The dark photon,” (2020), arXiv:2005.01515 [hep-ph].
- [9] J. Blumlein, *Prog. Part. Nucl. Phys.* **69**, 28 (2013), arXiv:1208.6087 [hep-ph].
- [10] H. Abramowicz *et al.* (H1, ZEUS), *Eur. Phys. J.* **C75**, 580 (2015), arXiv:1506.06042 [hep-ex].
- [11] K. Kovak, P. M. Nadolsky, and D. E. Soper, (2019), arXiv:1905.06957 [hep-ph].
- [12] H1 and Z. Collaborations, “Combination of measurements of inclusive deep inelastic $e^\pm p$ scattering cross sections and qcd analysis of hera data,” (2015), arXiv:1506.06042 [hep-ex].
- [13] M. Tanabashi *et al.* (Particle Data Group), *Phys. Rev.* **D98**, 030001 (2018).
- [14] D. Clark, E. Godat, and F. Olness, *Computer Physics Communications* **216**, 126137 (2017).
- [15] S. Carrazza, C. Degrande, S. Iranipour, J. Rojo, and M. Ubiali, *Physical Review Letters* **123** (2019), 10.1103/physrevlett.123.132001.
- [16] J. L. Abelleira Fernandez, C. Adolphsen, A. N. Akay, H. Aksakal, J. L. Albacete, S. Alekhin, P. Allport, V. Andreev, R. B. Appleby, E. Arikan, and et al., *Journal of Physics G: Nuclear and Particle Physics* **39**, 075001 (2012).
- [17] R. A. Khalek, S. Bailey, J. Gao, L. Harland-Lang, and J. Rojo, *SciPost Physics* **7** (2019), 10.21468/scipostphys.7.4.051.
- [18] T.-J. Hou, J. Gao, T. J. Hobbs, K. Xie, S. Dulat, M. Guzzi, J. Huston, P. Nadolsky, J. Pumplin, C. Schmidt, I. Sitiwaldi, D. Stump, and C. P. Yuan, “New cteq global analysis of quantum chromodynamics with high-precision data from the lhc,” (2019), arXiv:1912.10053 [hep-ph].
- [19] J. Lees *et al.* (BaBar), *Phys. Rev. Lett.* **113**, 201801 (2014), arXiv:1406.2980 [hep-ex].
- [20] J. Lees *et al.* (BaBar), *Phys. Rev. Lett.* **119**, 131804 (2017), arXiv:1702.03327 [hep-ex].
- [21] R. Aaij *et al.* (LHCb), *Phys. Rev. Lett.* **120**, 061801 (2018), arXiv:1710.02867 [hep-ex].
- [22] M. Baumgart, C. Cheung, J. T. Ruderman, L.-T. Wang, and I. Yavin, *JHEP* **04**, 014 (2009), arXiv:0901.0283 [hep-ph]; R. Essig, P. Schuster, and N. Toro, *Phys. Rev. D* **80**, 015003 (2009), arXiv:0903.3941 [hep-ph].